ELSEVIER

Journal of Power Sources 103 (2002) 213–222

JOURNAL OF POWER SOURCES

www.elsevier.com/locate/jpowsour

Finite element (FE) modelling of current density on the valve regulated lead/acid battery positive grid

R.J. Ball[a,*], R. Evans[b], R. Stevens[a]

[a]Department of Engineering and Applied Science, University of Bath, Bath BA2 7AY, UK
[b]Invensys, Westinghouse Site, Chippenham, Wiltshire SN15 1SJ, UK

Received 30 March 2001; received in revised form 25 June 2001; accepted 29 June 2001

Abstract

During operation of the valve regulated lead/acid (VRLA) battery, a mixed stoichiometry lead oxide corrosion layer is formed on the surface of the positive electrode. The formation of this layer has a number of consequences including increased electrode resistance and decreased strength. Experimental results obtained from cycling 40 A h VRLA batteries revealed an increase in corrosion layer thickness on the sides of the grid bars compared to the top and bottom. It is suggested that the areas of increased corrosion layer thickness corresponded to the areas of high current density on the surface of the grid. In order to investigate this observation the finite element package ANSYS was used to produce qualitative estimates of the values in current density, which would be expected on the tested grid design. Results suggest that corrosion layer thickening is related to current density. The model was then used to predict the expected current distribution around a number of hypothetical electrode designs. These incorporated changes in both grid bar cross-section and positive active material. Results showed that improvements could be made to existing grid designs with respect to lowering current densities. © 2002 Elsevier Science B.V. All rights reserved.

Keywords: VRLA battery; Grid; Finite element analysis; ANSYS

1. Introduction

Valve regulated lead/acid (VRLA) battery cells, constructed using a flat plate design, consist of a number of interleaved electrodes, each comprising a lead grid surrounded by either positive or negative active material. The grid bar gives support to the active material, however, its primary function is to act as a current collector.

A large segment of the VRLA battery market is for cyclic applications; consequently cycle life is an important factor to consider when designing a battery. Electrode design can affect cycle life by determining the current profile during charge and discharge, which is related to efficiency. Battery designers have been aware of this for many years and inclusion of features such as additional grid bars directed towards the lug can be seen on many designs as a method of improving the efficiency of current collection in the plane of the electrode.

During battery operation electrons flow between the electrode grid and positive active material. The difference in surface area between the active material, approximately 500 m^2 and grid, approximately 50 cm^2, results in a large increase in current density at the grid/positive active material interface. Pavlov [1] has suggested that grid bar shape and plate design will influence the uniformity of current distribution on the grid surface. As a basic electrode design principle it is advantageous to have as low and uniform a current density as is practically possible. A model proposed by Pavlov suggests that the cycle life of positive plates depends on the variations in current density on the grid surface, as this determines the intensity of the destructive processes in the positive active mass during operation.

Unpublished work by the authors into the affects of cycling on positive grid/corrosion layer growth showed a thicker corrosion layer on the surfaces of the grid bar, where the maximum current density was expected. It is believed that a higher current density can lead to a raised temperature resulting from resistance heating.

Due to the complex geometry of the grid bar, calculating the variation in current density using an analytical method would be extremely complicated and practically impossible. A more practical approach is to use a finite element (FE) method to solve the problem. The package chosen to obtain a solution was ANSYS [2]. ANSYS is a multi-purpose FE

---

[*] Corresponding author. Tel.: +44-1225-826826;
fax: +44-1225-826098.
E-mail address: r.j.ball@bath.ac.uk (R.J. Ball).

PII: S0378-7753(01)00857-6

program that can be used to solve a number of physical problems including current flow in a material.

2. Battery manufacture and testing

The results presented in this paper are based on observations of corrosion layer thickness made on a number of test batteries. The battery design used is a 40 A h VRLA product, manufactured using grey oxide positive active material and grey oxide negative active material. 100% glass microfibre separators were used consisting of 70% coarse and 30% fine fibres.

Cycling was carried out automatically using Digitron charging units. Each cycle consisted of a constant current discharge at 7.05 A to 10.2 V followed by a constant voltage recharge at 14.7 V for 16 h. This was repeated until the capacity after charging reduced to less than 80% of the starting capacity. The cell that showed the greatest voltage difference between end of discharge and end of charge was examined as this cell exhibited the thickest positive grid/corrosion layer. In order to determine the positive grid/corrosion layer thickness plates were removed from the battery case, washed in distilled water, dried in a vacuum oven and then encapsulated in resin. Cross-sections of the grid bars were then prepared using standard materialographic grinding and polishing techniques. Images of the cross-sections were obtained using a Jeol 6310 scanning electron microscope after a thin layer of gold had been sputter coated onto the sample surface to prevent charging.

Examination of a range of batteries which failed after varying numbers of cycles, between 10 and 133 times, indicated that there was a greater thickening of the corrosion layer on the edge of the grid bars compared to the top and bottom. This observation was most clearly illustrated on the bad cell of the battery that sustained 92 cycles to failure. A photomicrograph showing the grid/corrosion in this cell is recorded later in this paper, for comparative purposes with the FE model.

3. Calculation of electron flow in a material

In order to use ANSYS to solve current conduction problems it is necessary to make the analogy with the heat transfer problems. ANSYS solves electrical problems as a heat flow problem and substitutions must be made for the input and output variables. The quantity of heat flowing, Q, within a material is proportional to the length of time, t, cross-sectional area, A, and temperature gradient, as shown in Fig. 1. The temperature gradient, between points A and B in the figure, can be expressed in terms of the two temperatures T_1, T_2 and the length, l, as shown in Eq. (1).

$$\frac{T_1 - T_2}{l} \tag{1}$$

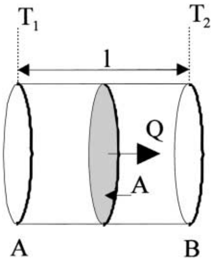

Fig. 1. Heat flow in a material.

As the heat flow, Q, is proportional to these quantities it can be expressed as

$$Q \propto tA\frac{T_1 - T_2}{l} \tag{2}$$

Therefore incorporating the thermal conductivity, K, Eq. (2) becomes

$$Q = KtA\frac{T_1 - T_2}{l} \tag{3}$$

When considering the electrical problem the current flow, I, is equal to the quantity of electrons flowing, Q, with time, t, as shown in Eq. (4).

$$I = \frac{Q}{t} \tag{4}$$

Current flow can also be related to potential difference, V, and resistance, R, by Ohm's law.

$$I = \frac{V}{R} = \frac{V_1 - V_2}{R} \tag{5}$$

And resistance can be written in terms of resistivity, ρ, length and area by

$$R = \frac{\rho l}{A} \tag{6}$$

Therefore by combining Eqs. (4)–(6), Eq. (7) is obtained:

$$Q = \frac{1}{\rho}tA\frac{V_1 - V_2}{l} \tag{7}$$

From the equations describing thermal (3) and electrical (7) behaviour, the thermal conductivity, K, is seen to be analogous to the electrical conductivity $1/\rho$. This allows an electrical problem to be solved in a thermal context if the substitution of input and output variables shown in Table 1 is made. The equations stated above for electrical and heat conduction are for one-dimensional (1-D) cases, however, in

Table 1
Substitution of input and output variables

	Thermal (ANSYS)	Electrical equivalent	Symbol
Input variable	Temperature	Potential (voltage)	Φ
	Heat generation	Current influx	Q
	Thermal conductivity	Electrical conductivity	K
Output variable	Sum of thermal flux	Current density	TF

the instance of the battery electrode it is necessary to generate a solution for 2-D or 3-D problems. ANSYS solves 2-D and 3-D problems by applying the Laplace equation [3]. This equation can be used for solving a wide range of continuous physical processes including, heat conduction and the distribution of electric potential. The equation can be written in its most basic form as shown below:

$$\frac{\partial}{\partial x}\left(k_x\frac{\partial \Phi}{\partial x}\right)+\frac{\partial}{\partial y}\left(k_y\frac{\partial \Phi}{\partial y}\right)+\frac{\partial}{\partial z}\left(k_z\frac{\partial \Phi}{\partial z}\right)+Q=0 \qquad (8)$$

where Φ is an unknown function assumed to be a single value within the region and k_x, k_y, k_z, and Q are known specified functions of x, y and z, respectively. For more detailed information on the solution techniques used to solve this equation the ANSYS guides [4] should be consulted.

4. Meshing of the geometry

In order to find the FE solution to a problem, it is first necessary to input the geometry of the component to be analysed into the package. After this step has been completed, the geometry is divided into smaller sections, called elements, which form a mesh. The mesh size and element shape, are predefined before the geometry is meshed. A finer mesh with smaller elements provides a more accurate solution compared to a coarser mesh as is illustrated in Fig. 2.

Solution accuracy is also influenced by element type. Generally elements can be defined in terms of their shape and the number of nodes or integration points. Larger numbers of integration points allow a more accurate solution for a given size of element. For the purposes of this analysis, a 2-D model utilising 2-D flat elements was used.

An advantage of using a coarse mesh and simple element is a reduction in the time taken by the computer to calculate the solution. For the size of the geometries modelled in this instance, even the most finely meshed condition only took ANSYS seconds to calculate an answer, therefore there was little advantage to using a coarser mesh. The element type used was a 2-D four-node quadrilateral solid element, referred to in the ANSYS guide as PLANE55. In order to ensure consistency of results, element and mesh size were kept the same for all calculations.

5. ANSYS output

Once the solution to a problem is obtained, post processing in ANSYS allows calculation of thermal flux (TF) in each direction. This can be calculated at the centre of each element or at the nodes. The output command used was 'sum of TF' which is calculated using the values of TF in each of the three directions: x, y and z, using Eq. (9). Since the model of the grid is 2-D, TF_z, can be assumed to be zero.

$$\mathrm{TF}_{\mathrm{SUM}}=\sqrt{|\mathrm{TF}_x|^2+|\mathrm{TF}_y|^2+|\mathrm{TF}_z|^2} \qquad (9)$$

The net sum of TF, $\mathrm{TF}_{\mathrm{SUM}}$, is represented in the form of a

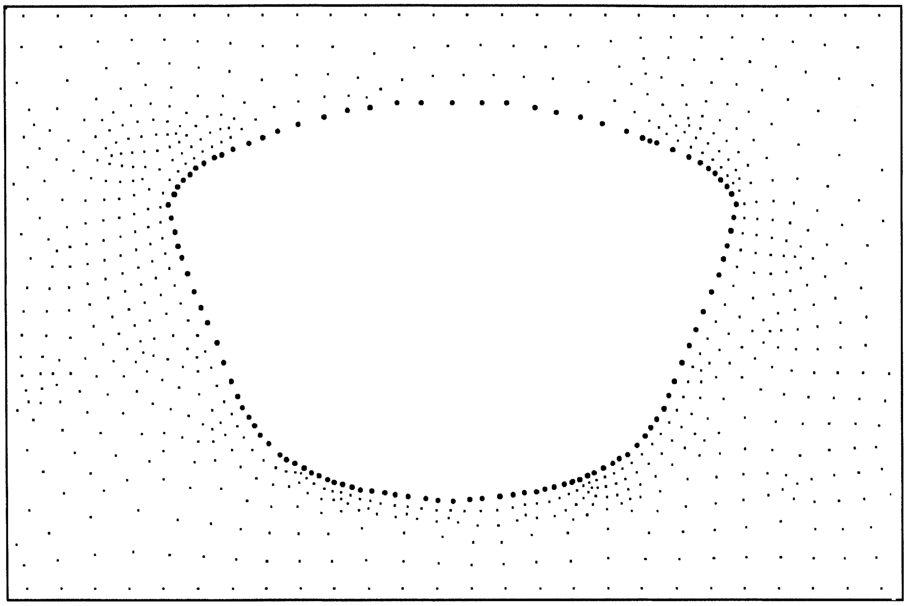

Positions of nodes are represented by dots on the diagram
Large dot (•) = Node where a constant temperature (or potential) is applied
Small dot (·) = Node where constant heat generation rate (or current influx) is applied

Fig. 3. Application of loads onto nodes of meshed geometry (positions of nodes are represented by dots on the diagram: large dot (•), node where a constant temperature (or potential) is applied; small dot (·), node where constant heat generation rate (or current influx) is applied).

contour plot. Positions of contour lines are determined from the flux gradient of the surrounding area and do not correspond to the positions of elements or nodes where the fluxes are calculated.

6. Application of Input variables into the model

When the component geometry is defined and meshed, temperatures and heat generation rates are applied onto the nodes. Nodes defining the edge of the grid bar are set at a constant temperature (potential), while heat generation (electron flux) is applied to the remaining nodes. This is shown diagrammatically in Fig. 3. For the analysis, properties of the active material are assumed to be isotropic, requiring the ‘isotropic material properties’ option within ANSYS to be used when inputting a value for conductivity.

7. Assumptions

The flow of electrons between the positive active material and lead grid, during operational life of a battery, is influenced by a range of factors. It is neither necessary nor practical to include all of these in the model. However, in order to exclude these a number of assumptions need to be made, details of which are given in the following paragraphs.

- Active material conductivity

  During discharge of the positive electrode lead dioxide is converted into lead sulphate. Lead sulphate is an insulator, therefore the proportion of the plate consisting of lead dioxide reduces during discharge and the resistance of the active material increases accordingly. However, this reaction does not occur uniformly throughout the bulk of the active material, so variation of conductivity with position relative to the grid bar and electrode surface may also occur. Any attempt to incorporate these changes into the model would prove to be highly problematic and for this reason it is assumed that the conductivity of the active material is constant and uniform throughout the electrode.
- Active material cracking

  Cracks are often observed within the bulk of the active material and at the grid/corrosion layer and corrosion layer/active material interfaces. Cracking will influence current density, as current flow will concentrate in areas of good electrical contact adjacent to a cracked region. Cracks form between the grid and positive active material during curing, or as a result of stresses caused by the changing dimensions of the active material while cycling. The geometry of the grid will influence the formation of cracks to a certain extent as sharp corners can act as areas of stress concentration, however, variations in current density are unlikely to be a significant contributor to the formation of cracks. It would be extremely hard to reliably predict where cracks may form relative to the grid bar and for this reason they are not included in the model.
- Corrosion layer

  The corrosion layer is not integral to the model. When the corrosion layer is uniform it will not influence current density and can therefore be excluded. However, variations in corrosion layer thickness will influence current density. Obtaining reliable values of the thickness in order to enter would be extremely difficult and would not contribute significantly in determining the best grid design.

Table 2
Quantities inputted into ANSYS model

Variable	Variable value entered into model
Constant temperature node	0
Constant heat generation	1
Isotropic conductivity	1

8. Selection of input variables

The fundamental difference between the model and battery electrode is that the input variables entered in the model are constants, whereas in the battery they vary depending on parameters such as discharge rate and depth of discharge. This makes quantitative estimation of actual current density values extremely difficult. However, the aim of this investigation is to evaluate the relative performance of different grid designs and this can be done if variables are kept constant. For this reason all geometries of the grids analysed are to the same scale and have the same loads applied, with the result that all variations in the solutions are a consequence of geometrical differences alone. The actual values entered into the ANSYS model are shown in Table 2.

9. Interpretation of a 2-D model representing a 3-D problem

The positive electrode is a 3-D component of the battery consisting of a lead grid surrounded by current producing positive active material. The task of inputting the geometry of the grid and active material into ANSYS can be simplified by considering the problem in two dimensions only. The 2-D sections of the electrode can be taken, in the plane of, or perpendicular to the orientation of the electrode. Fig. 4 shows a 3-D representation of a small section of positive electrode with the sections marked.

The actual cross-sectional shape of the grid bar is not square, as shown in the diagram above, but is a trapezoidal shape with curved edges. It is therefore symmetrical in the vertical plane but not in the horizontal. If the ‘in-plane’ section is modelled a certain amount of flux would flow in the z-direction (out of the paper), however, the flux in the

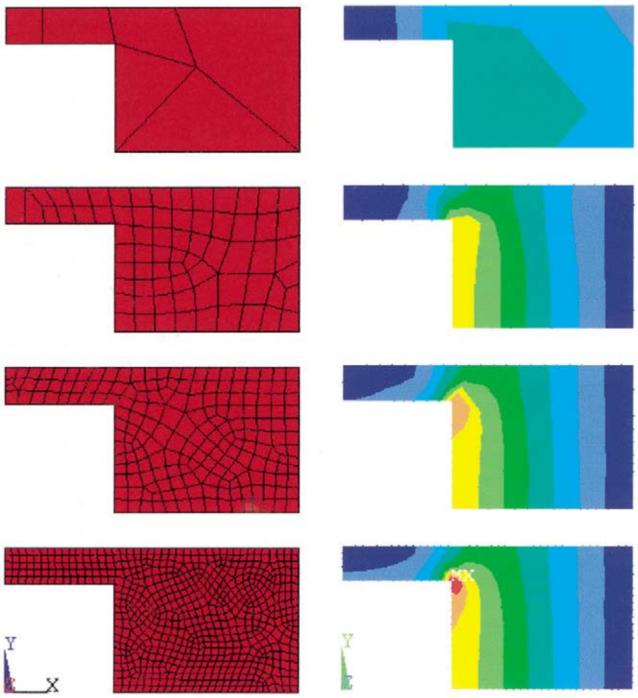

Fig. 2. Effect of mesh size on FE solution (coarse mesh, top/fine mesh, bottom).

x- and *y*-directions can be predicted. Fig. 5 shows the variations in current density for a grid hole.

The current density pattern shown in the diagram is symmetrical about the centre line, indicating that on this line there is a flux in the vertical direction but not in the horizontal. It follows that if a perpendicular slice of the electrode is modelled in this position the net flux in the *z*-direction will be zero and the model will be representative.

10. Evaluation of current grid design

During electrode manufacture the grid is coated in a layer of positive paste which is transformed to positive active material during battery formation. For the purposes of this study an electrode thickness of 1 mm was used. In order to model a component it is only necessary to enter a single repeating unit of the structure. The shaded area in Fig. 6 represents a suitable unit for the current grid design. This area was chosen as it allows a non-symmetrical shape of grid bar to be modelled.

A typical cross-section from the bad cell of a battery cycled 92 times is shown in Fig. 7. A uniform corrosion layer is visible around the top and bottom surfaces of the bar,

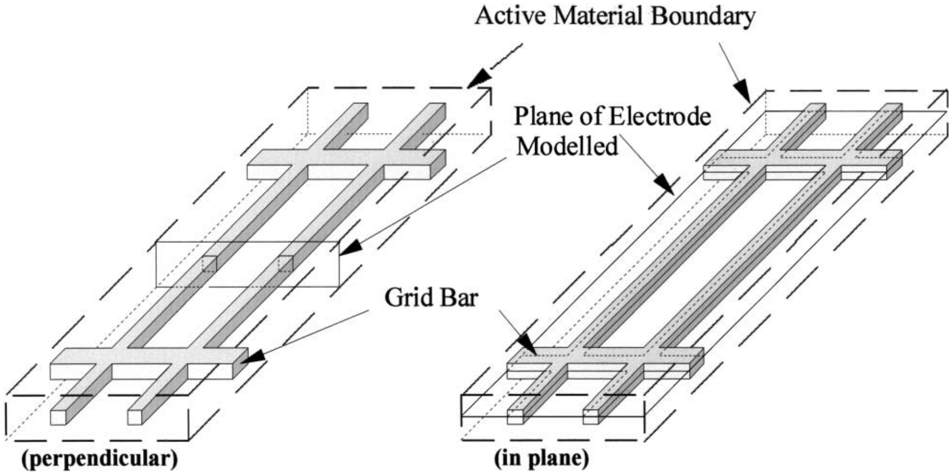

Fig. 4. Sections taken when modelling positive electrode.

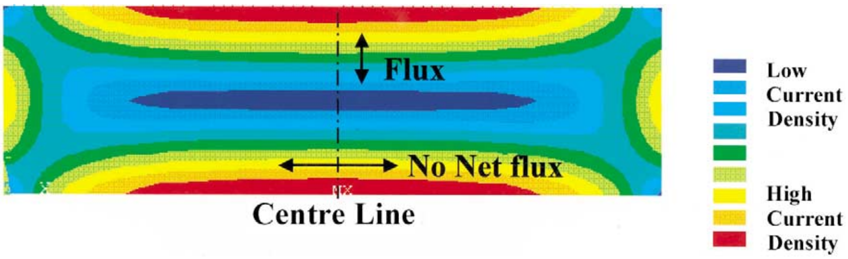

Fig. 5. Variations in current density for a grid hole.

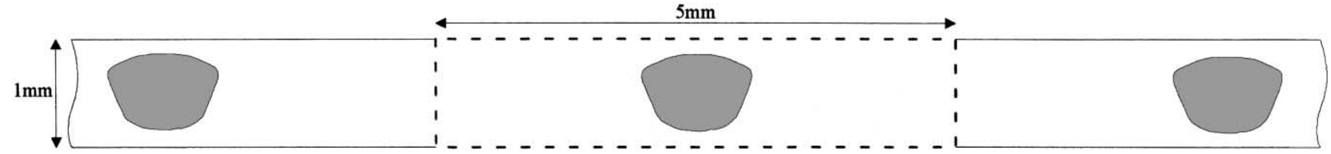

Fig. 6. Positive electrode cross-section showing area modelled.

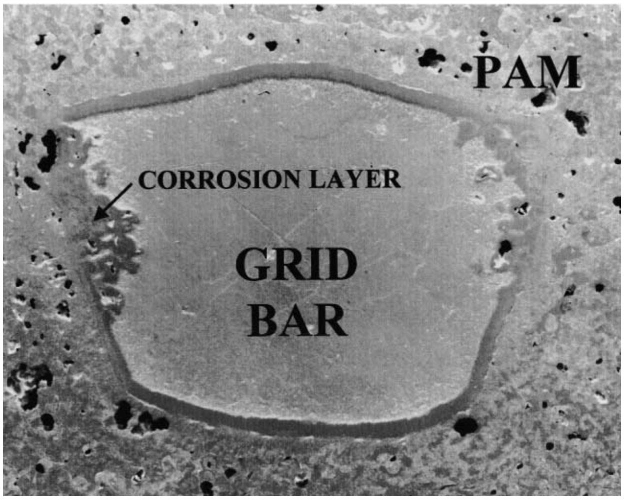

Fig. 7. Cross-section of grid bar showing thickening of corrosion layer.

however, substantial thickening of the layer has occurred on the upper section of the sides.

The variation in current density produced when the geometrical arrangement of the grid bar shown in Fig. 7 is entered into ANSYS is shown in Fig. 8a and b. Fig. 8a shows a cross-section of grid bar with surrounding positive active material and Fig. 8b is a close-up of the grid bar showing the current density around the surface of the grid bar. It is apparent that the areas having high values of the corrosion layer thickness in Fig. 7 correspond to the areas of high current density shown in Fig. 8.

11. Effect of grid bar orientation on current density distribution

During the grid production and pasting processes involved in battery manufacture, grid bars can sometimes become rotated about their central axis. This can result in a variation in current density distribution around the grid bar surface. Fig. 9 shows the current density distribution around two grid bars, orientated at 0 and 40°, respectively.

The variations in current density distribution can be compared more easily if the normalised current density is plotted against distance around the grid bar, shown diagrammatically in Fig. 10.

On the basis of current theory the curves shown in Fig. 10 would be expected to be smooth, however, they each contain a number of perturbations. This is caused by inconsistencies due to the mesh size and can be ignored. In comparing the curves, the effect of rotating the grid bar is to reduce the maximum current densities on each side. Grid bar orientation is therefore not an important factor and would not be expected to affect adversely battery performance in terms of corrosion layer growth.

12. Grid bar modification

In order to reduce the probability of a thick corrosion layer forming on the surface of the positive electrode grid, the current density on the surface must be as low as possible. This can be achieved by modifying the electrode to produce a uniform distribution and as low a current density as possible. One approach to achieve this is to modify the geometrical arrangement of the grid and active material. However, geometrical alterations to the design will have implications with regard to battery manufacturing method, performance and cycle life, etc. In addition to current density a number of additional conditions must be considered, details of which are given in the following section.

- Mechanical strength

  During manufacture the grid is rolled, pasted and cut into individual electrodes. These processes put the grid under mechanical stresses unlike those generated during battery operation. Any grid design must be able to withstand such stresses.
- Mechanical stability during corrosion

  As a battery grid corrodes the lead is converted into lead oxides of varying oxygen content. The consequential reduction of the grid bar cross-section, results in a decrease of mechanical strength and electrical conductivity. Consideration must therefore be given to the remnant strength of the grid bar after a certain amount of surface corrosion has occurred.
- Grid weight

  For many batteries weight is an important factor and it is advantageous to have as light a grid as possible.

When comparing different electrode designs any variation in current density must be a consequence of grid design only and not of size. To ensure all designs could be compared with each other the grid and active material cross-sectional areas were kept the same as that of the original electrode.

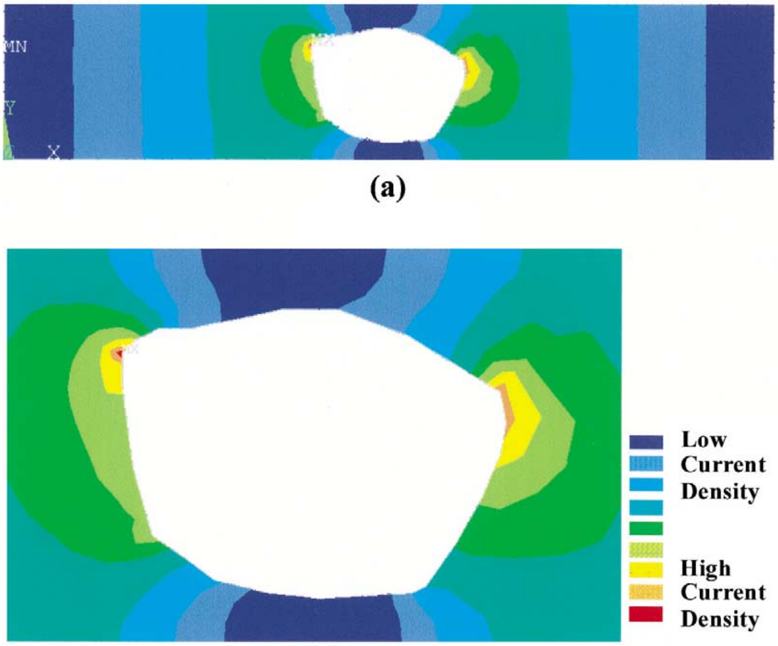

(a)

(b)

Fig. 8. Current density distribution around a battery grid bar.

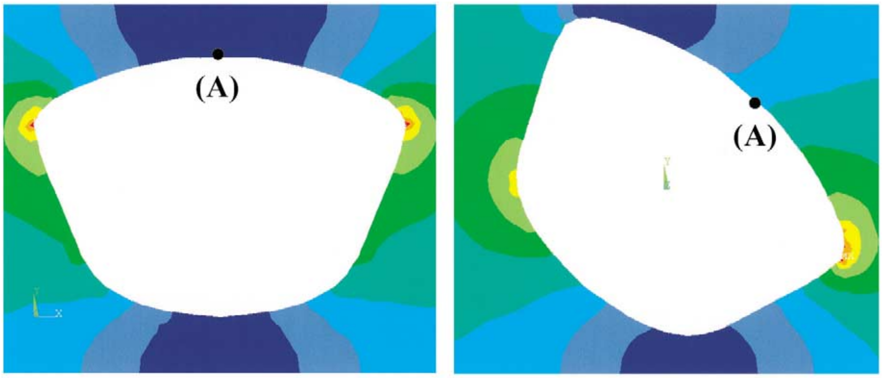

(Orientation = 0°)

(Orientation = 40°)

Fig. 9. Effect of grid bar rotation on current density.

Dimensions of the grid designs used in the investigation are given in Table 3.

Current density distributions around the grid bar for each of the designs in Table 3 are shown in Fig. 11. Plotting the normalised current density against distance around the grid allows the magnitude of the current densities to be compared more easily, as shown in Fig. 12. From the figure it can be seen that there are differences in the value of current

Table 3
Dimensions of grid designs investigated

Design	Dimensions (mm)	CSA (mm^2)	Circumference (mm)	Normalised circumference
Circle (diameter)	0.82	0.54	2.58	0.95
Square (width)	0.74	0.54	2.94	1.08
Hexagon 0 (width)	0.79	0.54	2.74	1.01
Hexagon 30 (width)	0.79	0.54	2.74	1.01
Hawker energy (height)	0.7	0.54	2.71	1
Design (width)	1			

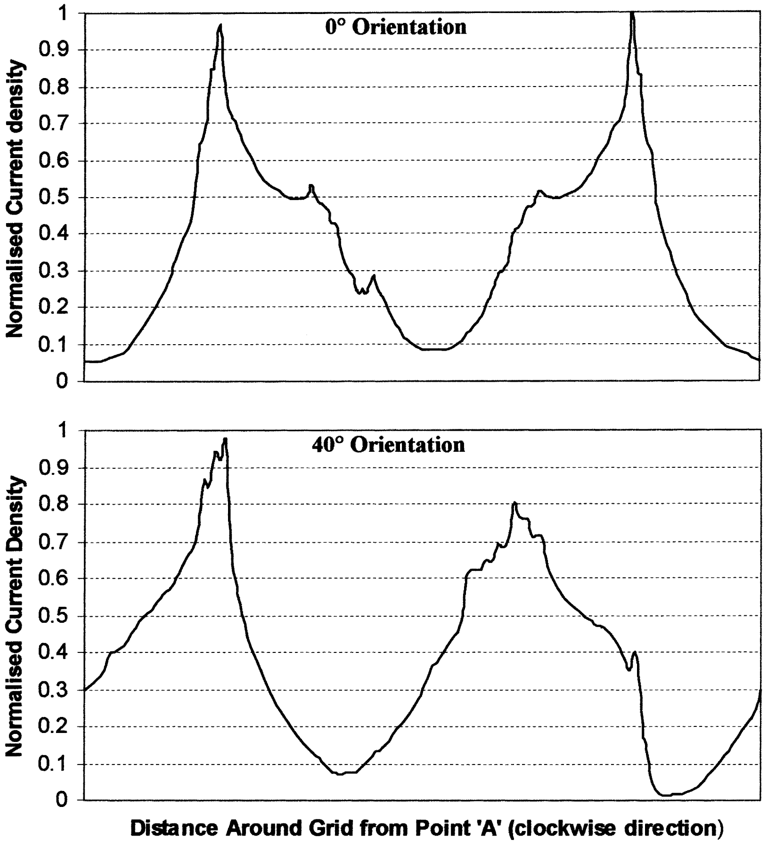

Fig. 10. Current density vs. position around grid bar.

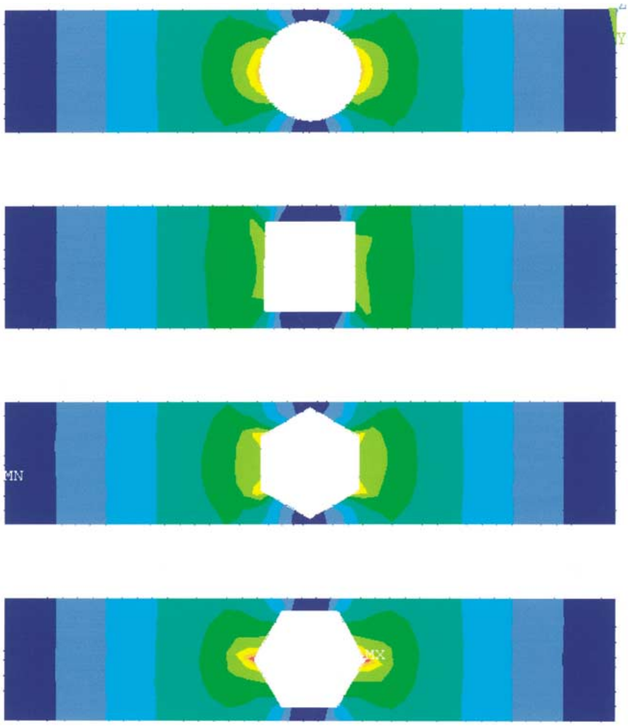

Fig. 11. Current density around new grid cross-sections.

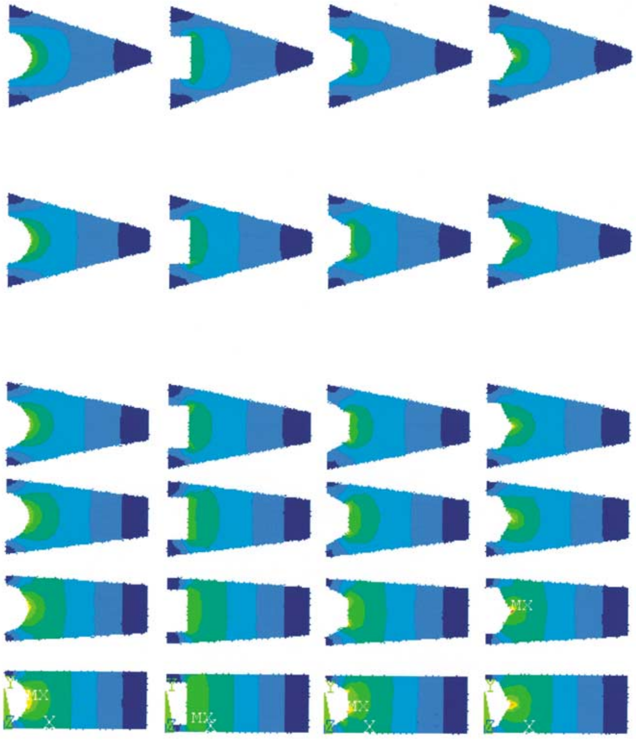

Fig. 13. Effect of positive active material geometry on current density distribution around grid bar.

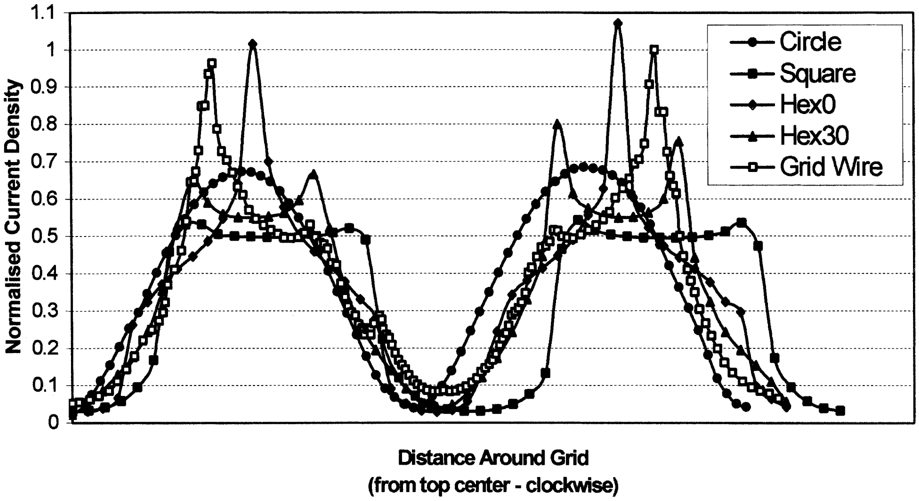

Fig. 12. Variations in current density on surface of different grid designs.

density obtained on each side of the bar. These can be accounted for by variations in the meshing generated by the computer. The maximum current density was obtained from the 0° orientated hexagon, followed by the original grid design, 30° orientated hexagon, circle and square. This is an interesting result as the relatively 'pointed' corners of the square do not appear to affect the current density significantly and the circle, which does not contain any 'pointed' surfaces, produces a higher maximum current density. This result highlights the influence of the amount of active material that surrounds the grid surface and suggests that re-arranging the geometry of the active material could be a much more effective method of reducing current density.

13. Effect of changing positive active material geometry

To investigate the effect of modifying the active material distribution around the grid bar a series of models were set-up where these changes were represented. Contour plots for a range of positive active material distributions are shown in Fig. 13.

The effect of increasing the amount of active material on the top and bottom of the grid bar is clearly evident. It can be seen that increasing the amount of active material in this way increases proportionally the current density in these regions, resulting in a decrease of the peak current density at the sides of the grid bar where the maximum values formerly occurred.

A cross-section through a hypothetical battery design implementing this principle is shown in Fig. 14. In order to implement this arrangement it can be seen that it is necessary to offset the grid bars in the positive and negative electrodes relative to each other. Although there would be clear advantages, as described, in adopting this arrangement, there are likely to be practical problems in implementing this concept where grid bars run in an orthogonal arrangement. One possible solution would lie in the construction of a battery where the grid bars ran in one direction only. The effect of this on the assembled electrode stiffness and strength, and the implications for a completed

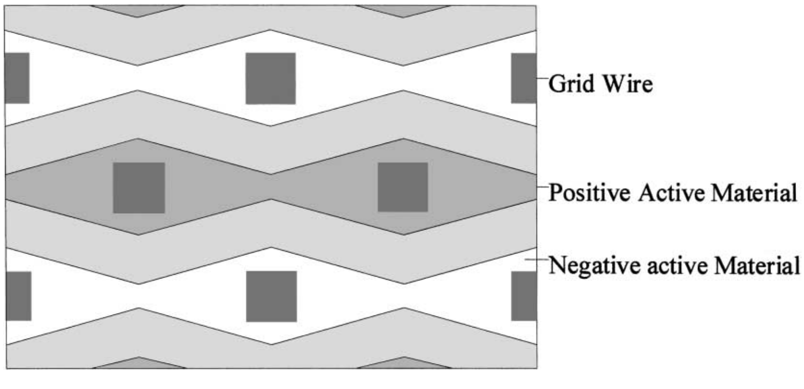

Fig. 14. Cell design to reduce current density.

battery would need to be assessed. It is suggested that considerable mechanical stiffness would be lost with this configuration.

14. Conclusions

The following conclusions can be drawn from the investigations.

1. Grid bar and positive active material geometry affect corrosion layer thickness.
2. Rotation of grid bars does not result in an increased current density distribution on the bar surface.
3. Current density distribution is greatly affected by grid shape.
4. Due to the uneven distribution and thickness of positive active material around the grid bar, a design with sharp corners such as a square section, does not necessarily result in the maximum current density distribution occurring at the corner of the square.
5. Changing the geometry of the positive active material surrounding the grid bar can have a significant effect on reducing the current density distribution.

Acknowledgements

Engineering and Physical Sciences Research Council support in the form of a studentship is acknowledged.

References

[1] D. Pavlov, A theory of the grid/positive active-mass (PAM) interface and possible methods to improve PAM utilisation and cycle life of lead/acid batteries, J. Power Sources 53 (1995) 9–21.
[2] ANSYS Inc., Southpointe 275 Technology Drive, Canonsburg, PA 15317.
[3] O.C. Zienkiewicz, The Finite Element Method in Engineering Science, McGraw-Hill, London.
[4] ANSYS Theory Reference, 8th Edition, SAS IP Inc.©, 000855, Chapter 6.